




Article

Disruption of Alternative Splicing in the Amygdala of Pigs Exposed to Maternal Immune Activation

Bruce R. Southey ¹, Marissa R. Keever-Keigher ¹, Haley E. Rymut ¹, Laurie A. Rund ¹,
Rodney W. Johnson ^{1,2,3} and Sandra L. Rodriguez-Zas ^{1,2,3,4,*}

¹ Department of Animal Sciences, University of Illinois at Urbana-Champaign, Urbana, IL 61801, USA; southey@illinois.edu (B.R.S.); keever1@illinois.edu (M.R.K.-K.); hrymut2@illinois.edu (H.E.R.); larund@illinois.edu (L.A.R.); rwjohn@illinois.edu (R.W.J.)

² Neuroscience Program, University of Illinois at Urbana-Champaign, Urbana, IL 61801, USA

³ Carl E. Woese Institute for Genomic Biology, University of Illinois, Urbana, IL 61801, USA

⁴ Department of Statistics, University of Illinois at Urbana-Champaign, Urbana, IL 61801, USA

* Correspondence: rodrzszs@illinois.edu

Abstract: The inflammatory response of gestating females to infection or stress can disrupt gene expression in the offspring's amygdala, resulting in lasting neurodevelopmental, physiological, and behavioral disorders. The effects of maternal immune activation (MIA) can be impacted by the offspring's sex and exposure to additional stressors later in life. The objectives of this study were to investigate the disruption of alternative splicing patterns associated with MIA in the offspring's amygdala and characterize this disruption in the context of the second stress of weaning and sex. Differential alternative splicing was tested on the RNA-seq profiles of a pig model of viral-induced MIA. Compared to controls, MIA was associated with the differential alternative splicing (FDR-adjusted p -value < 0.1) of 292 and 240 genes in weaned females and males, respectively, whereas 132 and 176 genes were differentially spliced in control nursed female and male, respectively. The majority of the differentially spliced (FDR-adjusted p -value < 0.001) genes (e.g., SHANK1, ZNF672, KCNA6) and many associated enriched pathways (e.g., Fc gamma R-mediated phagocytosis, non-alcoholic fatty liver disease, and cGMP-PKG signaling) have been reported in MIA-related disorders including autism and schizophrenia in humans. Differential alternative splicing associated with MIA was detected in the gene MAG across all sex-stress groups except for unstressed males and SLC2A11 across all groups except unstressed females. Precise understanding of the effect of MIA across second stressors and sexes necessitates the consideration of splicing isoform profiles.

Keywords: alternative splicing; maternal immune activation; weaning stress; sex; neurodevelopmental disorder



Citation: Southey, B.R.; Keever-Keigher, M.R.; Rymut, H.E.; Rund, L.A.; Johnson, R.W.; Rodriguez-Zas, S.L. Disruption of Alternative Splicing in the Amygdala of Pigs Exposed to Maternal Immune Activation. *Immuno* **2021**, *1*, 499–517. <https://doi.org/10.3390/immuno1040035>

Academic Editor: Marcella Reale

Received: 22 September 2021

Accepted: 16 November 2021

Published: 19 November 2021

Publisher's Note: MDPI stays neutral with regard to jurisdictional claims in published maps and institutional affiliations.



Copyright: © 2021 by the authors. Licensee MDPI, Basel, Switzerland. This article is an open access article distributed under the terms and conditions of the Creative Commons Attribution (CC BY) license (<https://creativecommons.org/licenses/by/4.0/>).

1. Introduction

Infections or other immune challenges during gestation result in the release of inflammatory signals that can reach the developing fetus. These signals can disrupt the offspring's molecular mechanisms [1–3] and have been associated with neurodevelopmental, neurodegenerative, immunological, metabolic, and behavioral disorders in humans and model organisms [4–9]. Moreover, MIA can alter the response to a challenge that the offspring may experience later in life [10,11]. Maternal immune activation (MIA) has been associated with autism spectrum disorder (ASD) [1,12,13], schizophrenia spectrum disorder (SSD), [14–17], Alzheimer's disease (AD) [18,19], and amyotrophic lateral sclerosis (ALS) [17,20,21].

The effects of MIA on the amygdala may influence the offspring's neuroendocrine profiles, social and sexually dimorphic behaviors, cognition, and the response to stressors [22,23]. Using a pig model of MIA elicited by a live virus, we reported that three-week-old pigs presented changes in the expression pattern of genes annotated to neurodevel-

opmental disorders, ASD, and SSD in the amygdala [24,25]. Subsequent investigations of the impact of the first challenge by MIA followed by weaning stress at three weeks of age confirmed the higher blood cortisol levels in weaned pigs relative to nursed pigs [7] and uncovered the potential modulating impact of MIA on the effects of weaning on genes annotated to autoimmune diseases and cell adhesion molecules [3]. Lipopolysaccharide (LPS)-elicited MIA in mice led to amygdala dysregulation in fetal and young adult offspring and increased pro-inflammatory markers [26], while MIA elicited by the synthetic viral agent polyinosinic:polycytidylic acid (Poly(I:C)) increased the synaptic strength of glutamatergic projections from the prefrontal cortex to the amygdala in mice [27].

Alternative splicing is prevalent in the brain [28,29], and the distinct transcript isoforms from a gene produced by alternative splicing can differ in function [30,31]. Changes in alternative splicing patterns were detected in MIA-related disorders, including ASD [32] and SSD [33,34]. The effects of MIA on the relative abundance of the isoforms in the amygdala are incompletely understood, and the variation in MIA effects on alternative splicing in the presence of a second stressor or across sexes remains uncharacterized.

A study of the effect of MIA on alternative splicing patterns in the offspring's amygdala was undertaken. Differential alternative splicing between virus-elicited MIA and control pigs was compared between females and males and between stress-exposed or unexposed individuals. The identification of differentially spliced genes and associated pathways and characterization of the splicing patterns supports an accurate understanding of the effects of MIA at the isoform level and precise identification of molecular targets for treatment.

2. Materials and Methods

2.1. Animal Experiments

The experiments were reviewed by the University of Illinois Institutional Animal Care and Use Committee (IACUC) in compliance with the NIH Public Health Service Policy on the Humane Care and Use of Animals and the USDA Animal Welfare Act. The experimental procedures were previously described [3], and the animal and molecular procedures that can influence the results from the alternative splicing analysis are highlighted.

At gestation day 69, gilts of Camborough breed (PIC, Hendersonville, TN, USA) and inseminated with semen from PIC 359 boars (PIC, Hendersonville, TN, USA) were moved into individual containment chambers. Gilts were used to minimize the likelihood of exposure to inflammatory challenge in previous parities. After a one-week adaptation period, and at the start of the final third of gestation, four gilts were inoculated intranasally with the live *Arteriviridae* porcine reproductive and respiratory virus (PRRSV), whereas a control group of four gilts was inoculated with sterile basal Dulbecco's modified Eagle medium. Gilts inoculated with PRRSV experienced a significant increase in body temperature and decrease in daily intake that dissipated by day 90 of gestation. The gilts were induced on day 113 of gestation such that the piglets were full-term born and remained with the gilt until 21 days of age when half of the pigs from each viral challenge group (MIA and control groups) were weaned and the rest of the pigs remained with the gilt (weaned and nursed groups, respectively). Weaned pigs were moved to separate chambers, in groups of 4 to 5 pigs, gilts and pigs were maintained at 22 °C with a 12-h light/dark cycle, had *ad libitum* water access, and were fed a diet that matches nutritional requirements. The blood cortisol level was higher in weaned pigs relative to nursed pigs [9]. The sample size per maternal challenge (MIA or control), second stress of weaning (weaned or nursed), and sex (female or male) group were $n = 6$, totaling 48 pigs studied. The pigs were anesthetized and euthanized at 22 days, peripheral blood drawn, and brain extracted. Blood analysis demonstrated higher stress indicator cortisol levels in weaned compared to nursed pigs [7].

The amygdalae were dissected from the brains, flash-frozen, and stored at $-80\text{ }^{\circ}\text{C}$ until the RNA was isolated using the EZNA kit (Omega Biotek, Norcross, GA, USA). Individual amygdalae had RNA quality indicator RIN > 7.5 and were sequenced into 150 nucleotide paired-end reads using a NovaSeq 6000 (Illumina Inc., San Diego, CA, USA). The quality indicator was high throughout all positions (Phred > 35), and the FASTQ-formatted files,

including the sequences and quality scores, are stored in the Gene Expression Omnibus database (experiment identifier GSE165059, reviewers' token: cfcnegeczvurfgb).

2.2. RNA Sequence Mapping and Alternative Splicing Analysis

The approximately 13 billion reads across 48 amygdalae included on average 69.1 million paired-end sequences per pig (standard deviation/mean < 0.13). The median alignment rate was 86%, and the median number of splice junctions was approximately 37 million per amygdala.

Paired-end reads from the individual samples were aligned to the *Sus scrofa* genome version Sscrofa 11.1 using the software STAR v2.7.8a [35] in "twopassMode" so the novel junctions identified in the first alignment iteration are included in the second iteration [30]. The junction information was extracted from alignment files using RegTools [36], and unmapped junctions were removed from further analysis. The testing and visualization of the differential alternative splicing between MIA and control pigs used the software LeafCutter [37] using default settings (20 read minimum coverage, minimum of 3 samples per group and intron support present in at least 5 samples). LeafCutter uses exon-exon junction information from the sequence alignment against the genome to quantify and test for differential alternative splicing irrespective of the gene annotations. The differential splicing between MIA and control groups was interpreted based on the test *p*-value and the change in the proportion of splice site usage (Δ PSI) between groups for each intron cluster within a gene. Each intron cluster across exons defines a transcript isoform within a gene, and some splicing testing spanned genomic regions encompassing multiple genes [31]. Multiple sets of intron clusters and multiple differential splicing tests can encompass several genes. Therefore, on average, approximately 34,500 tests for differential splicing were performed across sex and weaning groups. The *p*-values also include a false discovery rate (FDR) adjustment for multiple testing across gene-intron clusters [38].

The identification of over-represented KEGG pathways among the differentially spliced genes (FDR *p*-value < 0.1) relied on the Database for Annotation, Visualization and Integrated Discovery tool (DAVID 6.8) [39]. The differential splicing threshold was selected in recognition that pathway components respond to conditions (e.g., MIA, weaning stress) in different magnitudes and that the genes in a pathway have varying isoform quantitation. The functional analysis considered all genes annotated to the genomic region presenting differential alternative splicing, with 97% of the events annotated to a single gene. The enrichment of KEGG pathways was assessed against the *Sus scrofa* genome as background, and the FDR-adjusted *p*-value was calculated using a one-tailed jackknifed Fisher hypergeometric exact test. The pathway enrichment was also characterized using the fold enrichment computed as the odds ratio between the proportion of pathway genes among the genes presenting differential splicing (FDR-adjusted *p*-value < 0.1) relative to the proportion of pathway genes in the *Sus scrofa* genome.

3. Results

The number of differentially alternatively spliced genes (FDR-adjusted *p*-value < 0.1) between the MIA and control groups was 132 in nursed females and 292 in weaned females. The genes presenting the most significant differential splicing (FDR-adjusted *p*-value < 0.001) in nursed and weaned females are listed in Table 1, along with the most extreme positive and negative Δ PSI, the unadjusted and FDR-adjusted *p*-values. The genes presenting the highest differential splicing in nursed females included ubiquitin carboxyl-terminal hydrolase 30 (USP30), protein kinase CAMP-dependent type I regulatory subunit beta (PRKAR1B), and NSFL1 cofactor p47 (NSFL1C), while the genes in weaned females included zinc finger protein 316 (ZNF316), SH3 and multiple ankyrin repeat domains 1 (SHANK1), actin binding LIM protein family member 3 (ABLIM3), heart development protein with EGF like domains 1 (HEG1), and multiple EGF like domains 8 (MEGF8).

Table 1. Genes presenting differential alternative splicing (FDR-adjusted p -value < 0.001) in response to exposure to maternal immune activation (MIA) relative to controls in the amygdala of nursed and weaned female pigs.

Gene Symbol	Extreme <0 Δ PSI ¹	Extreme >0 Δ PSI ²	Isoform Count ³	p -Value	FDR-Adjusted p -Value
<i>Nursed</i>					
NSFL1C	−0.116	0.021	9	3.02×10^{-15}	1.02×10^{-10}
PDK2	−0.036	0.041	7	1.94×10^{-14}	3.27×10^{-10}
USP30	−0.147	0.102	6	2.09×10^{-10}	2.35×10^{-6}
MAG	−0.019	0.010	4	4.48×10^{-8}	2.15×10^{-4}
NPTXR	−0.024	0.031	3	1.14×10^{-7}	4.78×10^{-4}
TAF1D	−0.037	0.028	18	1.68×10^{-7}	6.27×10^{-4}
SLC25A11	−0.018	0.018	3	2.14×10^{-7}	6.91×10^{-4}
ZNF513	−0.017	0.012	4	2.26×10^{-7}	6.91×10^{-4}
RIMS1	−0.025	0.030	17	3.31×10^{-7}	9.27×10^{-4}
PRKAR1B	−0.053	0.096	3	3.71×10^{-7}	9.60×10^{-4}
<i>Weaned</i>					
RPL28	−0.017	0.025	7	9.96×10^{-10}	7.07×10^{-6}
TYW3	−0.027	0.031	14	1.96×10^{-9}	1.16×10^{-5}
ADAP1	−0.009	0.007	6	5.26×10^{-9}	2.02×10^{-5}
ATP5H	−0.029	0.024	5	1.14×10^{-8}	3.66×10^{-5}
ZNF316	−0.224	0.081	6	1.29×10^{-8}	3.83×10^{-5}
SHANK1	−0.056	0.110	4	2.14×10^{-8}	5.85×10^{-5}
ACP6	−0.017	0.017	2	2.52×10^{-8}	6.40×10^{-5}
ABLIM3	−0.042	0.092	7	3.49×10^{-8}	8.26×10^{-5}
KCTD2	−0.005	0.010	3	3.87×10^{-8}	8.58×10^{-5}
HEG1	−0.121	0.115	5	5.86×10^{-8}	1.18×10^{-4}
CXCL14	−0.032	0.032	3	5.97×10^{-8}	1.18×10^{-4}
NAGK	−0.024	0.036	4	2.78×10^{-7}	4.79×10^{-4}
FAM213A	−0.008	0.015	3	2.84×10^{-7}	4.79×10^{-4}
TM7SF2	−0.006	0.010	11	4.03×10^{-7}	6.22×10^{-4}
VRK3	−0.027	0.048	7	4.79×10^{-7}	7.08×10^{-4}
ATP11B	−0.035	0.054	3	5.01×10^{-7}	7.11×10^{-4}
MEGF8	−0.087	0.053	3	7.10×10^{-7}	8.99×10^{-4}

¹ The extreme negative Δ PSI column quantifies the isoform that presented the highest under-expression in MIA relative to control female pigs. ² The extreme positive Δ PSI column quantifies the isoform that presented the highest over-expression in MIA relative to control female pigs expressed in proportion. ³ Isoform count indicates the number of isoforms in the gene presenting alternative splicing.

The number of differentially alternatively spliced genes (FDR-adjusted p -value < 0.1) between the MIA and control groups was 176 in nursed males and 240 in weaned males. The genes presenting the most significant differential splicing genes (FDR-adjusted p -value < 0.001) in nursed and weaned males are listed in Table 2. The genes presenting the highest differential splicing in nursed males included septin 7 (SEPT7), zinc finger protein 672 (ZNF672), and potassium voltage-gated channel subfamily A member 6 (KCNA6), while the genes in weaned males included ADP ribosylation factor like GTPase 4D (ARL4D), HOP homeobox (HOPX), and neurofilament medium chain (NEFM).

Table 2. Genes presenting differential alternative splicing (FDR-adjusted p -value < 0.001) in response to exposure to maternal immune activation (MIA) relative to controls in the amygdala of nursed and weaned male pigs.

Gene Symbol	Extreme $<0 \Delta$ PSI ¹	Extreme $>0 \Delta$ PSI ²	Isoform Count ³	p -Value	FDR-Adjusted p -Value
<i>Nursed</i>					
KCNA6	-0.052	0.068	11	1.34×10^{-11}	4.65×10^{-7}
GPBP1	-0.015	0.019	3	4.18×10^{-10}	7.24×10^{-6}
SEPT7	-0.315	0.305	3	1.22×10^{-9}	1.41×10^{-5}
ZNF672	-0.114	0.067	12	1.78×10^{-9}	1.54×10^{-5}
CNP	-0.005	0.005	6	1.18×10^{-8}	7.30×10^{-5}
GFAP	-0.008	0.017	6	1.26×10^{-8}	7.30×10^{-5}
ZNF74, DGCR2	-0.019	0.016	12	5.79×10^{-8}	2.87×10^{-4}
MYT1L	-0.027	0.053	11	1.62×10^{-7}	7.01×10^{-4}
<i>Weaned</i>					
ARL4D	-0.042	0.279	10	1.11×10^{-10}	2.01×10^{-6}
HNRNPA2B1	-0.040	0.053	6	2.63×10^{-10}	2.01×10^{-6}
PDK2	-0.041	0.045	7	2.72×10^{-10}	2.01×10^{-6}
CDC42	-0.055	0.037	4	3.29×10^{-10}	2.03×10^{-6}
HOPX	-0.087	0.108	12	4.33×10^{-10}	2.29×10^{-6}
POLR2E	-0.016	0.016	2	3.35×10^{-8}	1.38×10^{-4}
NCAN	-0.006	0.007	6	4.56×10^{-8}	1.69×10^{-4}
TCF25	-0.009	0.008	7	5.50×10^{-8}	1.85×10^{-4}
BBIP1	-0.022	0.013	15	6.68×10^{-8}	1.90×10^{-4}
CLU	-0.042	0.044	5	7.31×10^{-8}	1.93×10^{-4}
DRC7	-0.063	0.031	7	9.55×10^{-8}	2.30×10^{-4}
MSRA	-0.013	0.023	23	1.19×10^{-7}	2.52×10^{-4}
SEC61A2	-0.018	0.017	6	1.23×10^{-7}	2.52×10^{-4}
LAMTOR4	-0.015	0.009	8	1.47×10^{-7}	2.73×10^{-4}
BLOC1S1	-0.006	0.006	5	2.00×10^{-7}	3.41×10^{-4}
AMDHD1, SNRPF	-0.048	0.037	4	2.02×10^{-7}	3.41×10^{-4}
FAM213B	-0.027	0.016	8	3.72×10^{-7}	5.99×10^{-4}
NEFM	-0.097	0.132	13	5.81×10^{-7}	8.97×10^{-4}

¹ The extreme negative Δ PSI column quantifies the isoform that presented the highest under-expression in MIA relative to control female pigs. ² The extreme positive Δ PSI column quantifies the isoform that presented the highest over-expression in MIA relative to control female pigs expressed in proportion. ³ Isoform count indicates the number of isoforms in the gene presenting alternative splicing.

Figures 1 and 2 depict the relative abundance (proportion) of isoforms between MIA and control groups for genes presenting significant alternative splicing (FDR-adjusted p -value < 0.001 and $>10\%$ differential abundance between extreme over- and under-expressed isoforms) in females and males, respectively. The semicircles indicate the intron clusters corresponding to transcript isoforms where bold and thin red semicircles denote annotated and novel isoforms, respectively. The black boxes denote the gene exons and the superscript letters identify distinct isoforms.

Table 3 lists the genes that presented differential alternative splicing (FDR-adjusted p -value < 0.1) between MIA and control pigs in two or more groups that share stress or sex. Under weaning stress, females and males shared the highest number of differentially spliced genes (13 genes) between MIA and control groups, whereas nursed females and males shared the fewest differentially spliced genes (3 genes). Noteworthy is the differential splicing patterns of myelin associated glycoprotein (MAG) and solute carrier family 2 member 11 (SLC2A11). MAG presented differential alternative splicing in all groups except nursed males, and SLC2A11 presented differential alternative splicing in all groups except nursed females.

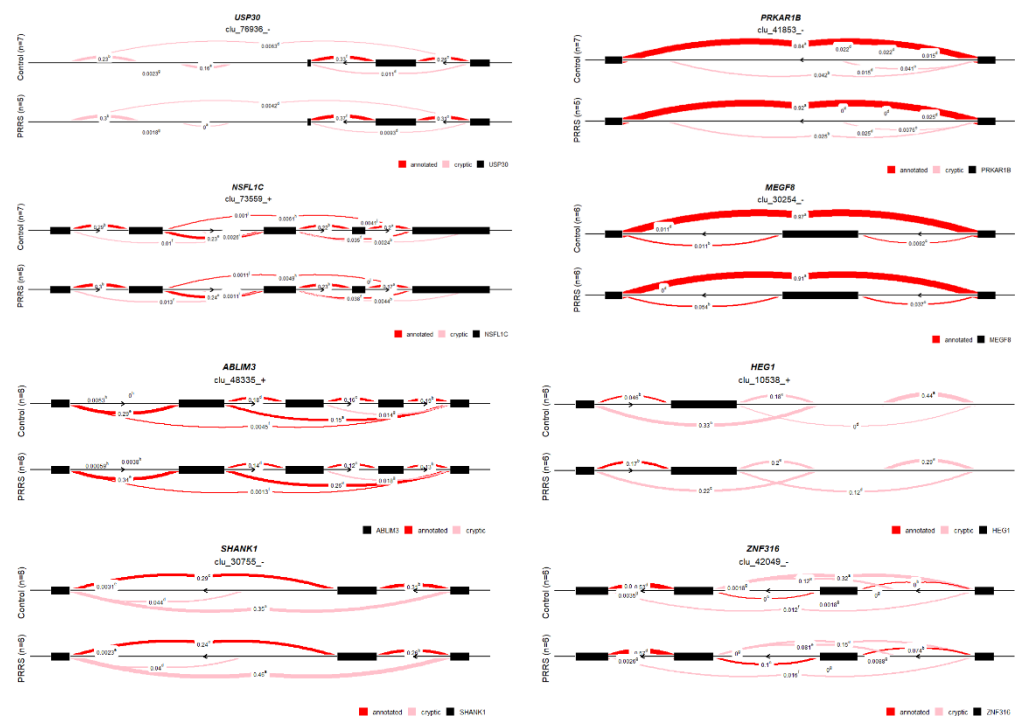


Figure 1. Genes presenting alternative splicing (False Discovery Rate-adjusted p -value < 0.001, >10% differential abundance between extreme over- and under-expressed intron clusters) among female pigs exposed to maternal immune activation (P or PRRSV-elicited MIA) versus unexposed (C or control). The semicircles indicate the intron clusters corresponding to transcript isoforms, where dark and soft red semicircles denote annotated and novel isoforms. The black boxes denote the gene exons and the superscript letters identify distinct intron clusters.

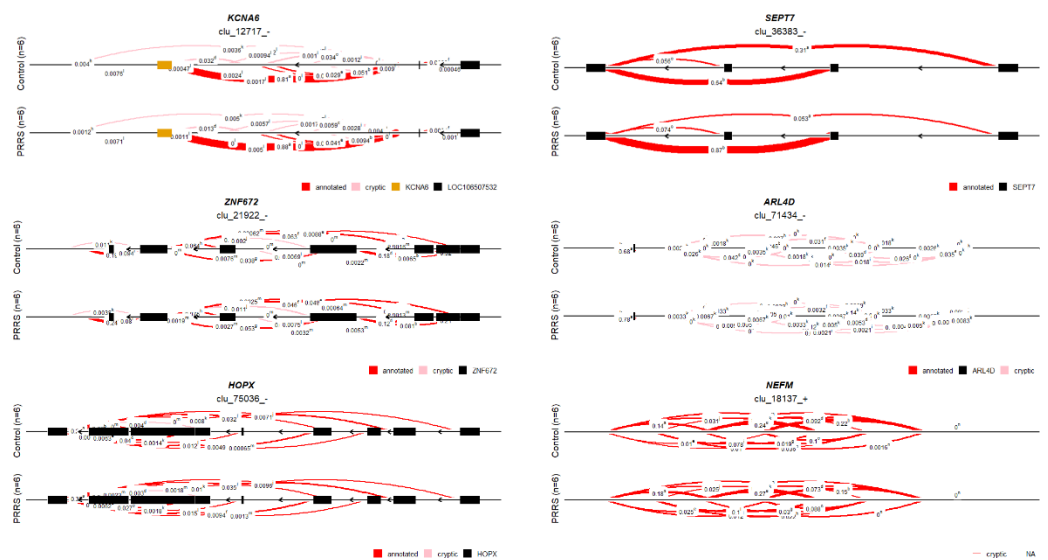


Figure 2. Genes presenting alternative splicing (False Discovery Rate-adjusted p -value < 0.001, >10% differential abundance between extreme over- and under-expressed intron clusters) among male pigs exposed to maternal immune activation (P or PRRSV-elicited MIA) versus unexposed (C or control). The semicircles indicate the intron clusters corresponding to transcript isoforms, where dark and soft red semicircles denote annotated and novel isoforms. The black boxes denote the gene exons and the superscript letters identify distinct intron clusters.

Table 3. Differential alternative spliced genes between maternal immune activation and control pigs shared among stress (weaned and nursed) and sex (female and male) groups.

Groups Compared	Gene Symbols Shared between Groups Compared ¹
Female weaned and nursed (9 genes)	LOC110261221, MAG, MAPK10, MARCKSL1, SPTAN1, TAF1D, TMEM9, TTYH1, TYW3
Male weaned and nursed (7 genes)	FAM13B, GIGYF2, KHK, KIAA0513, LZIC, SLC2A11, SYT17
Nursed females and males (3 genes)	EEF2, MIGA1, RIMS1
Weaned females and males (13 genes)	ABCA3, ACAP3, ATP5H, LOC100626407, LOC110261384, MAG, NEFM, PRKCZ, PTEN, SHANK1, SLC2A11, SMARCA2, WDR34

¹ MAG and SLC2A11 present differential splicing in three of the four groups studied.

Table 4 summarizes the KEGG pathways enriched at FDR-adjusted p -value < 0.1 by sex and weaning group among the genes presenting differential alternative splicing (FDR-adjusted p -value < 0.1) between MIA and control pigs by weaning stress and sex group. Enriched pathways among alternatively spliced genes included non-alcoholic fatty liver disease (ssc04932) in nursed females and metabolic pathways (ssc01100) in weaned males, while the most significant enrichment in weaned females was linoleic acid metabolism (p -value < 0.006, FDR-adjusted p -value > 0.1, fold enrichment = 10.5). Noteworthy is the highly significant enrichment of multiple functional categories among the alternatively spliced genes in nursed males including, cGMP-PKG signaling (ssc04022), dopaminergic synapse (ssc04728), amphetamine addiction (ssc05031), ribosome (ssc03010), and calcium signaling (ssc04020).

Table 4. Enriched KEGG pathways among genes presenting alternative splicing (False Discovery Rate-adjusted p -value < 0.1) associated with exposure to maternal immune activation by pig group.

Group and Path ID ¹	KEGG Pathway Name	Size ²	Enrichment Fold ³	p -Value
<i>Nursed Females</i>				
ssc04932	Non-alcoholic fatty liver disease (NAFLD)	4	5.15	0.039
ssc04666	Fc gamma R-mediated phagocytosis	3	7.53	0.056
ssc04144	Endocytosis	4	3.51	0.097
<i>Nursed Males</i>				
ssc04022	cGMP-PKG signaling pathway	6	5.02	0.006
ssc04728	Dopaminergic synapse	5	5.60	0.011
ssc05031	Amphetamine addiction	4	8.26	0.012
ssc03010	Ribosome	5	4.65	0.021
ssc04020	Calcium signaling pathway	5	3.71	0.042
<i>Weaned Males</i>				
ssc01100	Metabolic pathways	22	2.11	0.075
ssc05416	Viral myocarditis	5	8.96	0.103
ssc05332	Graft-versus-host disease	4	13.07	0.103
ssc05330	Allograft rejection	4	12.01	0.103
ssc04144	Endocytosis	8	3.78	0.103

¹ KEGG pathway identifier. ² Size = number of distinct genes in the pathway. ³ Enrichment fold = ratio between proportion of pathway genes in the significant splicing list relative to the genome.

4. Discussion

The differential alternative splicing associated with MIA uncovered in the amygdala offers insights into the transcriptional mechanisms that could explain the impact of in-

flammatory signals during development on postnatal physiology and behavior. Moreover, the detection of differential splicing profiles unique to the sex and experienced weaning stress advances the understanding of reports about MIA-associated disorders that present sex-dependent or stress-dependent incidence. Differential splicing findings are discussed at the gene and pathway levels in the context of transcriptomic and genomic reports on MIA-related and neurodevelopmental disorders.

Particularly noteworthy are genes MAG and SLC2A11 that presented differential alternative splicing between MIA and control pigs in three out of the four sex-stress groups studied (Table 3). SLC2A11 was differentially spliced between MIA and control pigs in all groups except nursed females with the highest MIA effect in weaned males (FDR-adjusted p -value < 0.03). A study of copy number variation in children with attention deficit hyperactivity disorder (ADHD) and patients with ASD [40] and a study of copy number variation in patients with SSD [41] identified regions encompassing SLC2A11 associated with these disorders.

The effect of MIA on the alternative splicing of MAG was detected in all groups except nursed males, and the highest differential splicing was detected in nursed females. The most and second most impacted isoforms were under- and over-expressed in MIA relative to control, respectively (Table 1, FDR-adjusted p -value < 0.0002). The identification of MAG isoforms that have opposite expression patterns in response to MIA is aligned with previous reports. Isoform bias in MAG has been proposed as an important factor in developing SSD [42]. While both short and long forms of MAG were under-expressed in the frontal cortex of SSD patients, long-form MAG was under-expressed to a greater extent, altering the ratio of short-form MAG to long-form MAG in SSD patients compared to controls [42].

The MAG isoform under-expressed in MIA pigs is in agreement with the reported under-expression of the long form of MAG in the amygdala of MIA mice exposed to the viral synthetic Poly(I:C) during gestation [43]. MAG was under-expressed in the prefrontal cortex of MIA rats exposed to Poly(I:C) during development [44], in the prefrontal cortex and nucleus accumbens of MIA mice exposed to Poly(I:C) during development [45], and in the cerebellum of mice exposed to influenza-elicited MIA [46]. On the other hand, the over-expression of a MAG isoform in MIA pigs (albeit less extreme than the previously discussed under-expressed isoform) is in agreement with the over-expression of MAG in the hippocampus of MIA offspring of Poly(I:C)-challenged rhesus macaques [47]. Our findings provide a possible explanation of the apparent contradiction in the MAG profiles associated with MIA.

Overall, 840 genes presented differential alternative splicing associated with MIA. The majority of the significant effects of MIA on alternative splicing were unique to particular sex-weaning stress groups with approximately 5% of the genes presenting differential splicing in multiple weaning-sex groups. Most genes presenting differential splicing in response to MIA were detected in pigs exposed to weaning stress while the distribution was fairly similar between sexes. Many of the genes differentially spliced between MIA and control pigs modulate signal transduction and synaptic plasticity, and these genes and pathways that have been previously associated with behavioral and neurodevelopmental disorders such as ASD and SSD. The limited overlap in genes impacted by MIA across pig groups suggests that an accurate and precise understanding of the effects of MIA on the molecular pathways requires the study of MIA at the transcript isoform level. Therefore, the effects of MIA are discussed within sex and stress group.

4.1. Differential Alternative Splicing Associated with Maternal Immune Association in Females

Several genes presenting differential alternative splicing associated with MIA in nursed females have been previously associated with MIA-related and neurodevelopmental disorders or conditions (Table 1). The most extreme isoforms of the gene TATA-box binding protein associated factor (TAF1D) were 3.7% under- and 2.8% over-expressed in MIA

relative to control nursed females. At the gene level, TAF1D was over-expressed in the prefrontal cortex of Poly(I:C)-elicited MIA offspring [45].

The differential alternative splicing of pyruvate dehydrogenase kinase 2 (PDK2) between MIA and control nursed females aligns with this gene's participation in pathways underlying synaptic strength in depression and spatial memory [48]. Moreover, the PDK2 protein participates in mTOR signaling and the dysregulation of this process contributes to impaired synaptic plasticity and ASD [49,50].

The pattern of alternative splicing for protein kinase CAMP-dependent type I regulatory subunit beta (PRKAR1B, Figure 1) includes highly over- and under-expressed intron clusters (9.6% and 5.3%, respectively) in MIA relative to control nursed females. In alignment with our findings, the differential expression profile of PRKAR1B between ASD patients and controls prompted the hypothesis that this gene is an ASD network hub [51].

The most extreme differential isoform of the neuronal pentraxin receptor (NPTXR) gene was over-expressed 3.1% in MIA relative to control nursed females and NPTXR was also over-expressed in the caudate gray matter of SSD patients compared to controls [52]. The 2.4% under-expression of a NPTXR isoform in MIA relative to control nursed females is aligned with a NPTXR knockout mice line that displayed behavioral deficits akin to those observed in MIA-associated disorders [53].

The differential splicing between MIA and control nursed females detected in the genes regulating synaptic membrane exocytosis 1 (RIMS1) and zinc finger protein 513 (ZNF513) may be linked to mutations in these genes that have been related to MIA-related phenotypes. Single-nucleotide polymorphisms in RIMS1 were associated with SSD and ASD incidence [54,55]. Likewise, polymorphisms in ZNF513 were associated with altered brainstem volume in patients diagnosed with ASD, SSD, ADHD, MDD, and bipolar disorder [56]. The differential alternative splicing of CALCB (p -value < 0.008) between MIA and control nursed females agrees with the identification of this neuropeptide precursor as a candidate gene for ASD in a rat model [57].

The most extreme differentially expressed isoforms of solute carrier family 25 member 11 (SLC25A11) between MIA and control nursed females had comparable over- and under-expression (| 1.8% |). The SLC25A11 isoform profiles detected in the present study may be associated with the range of profiles reported for this gene related to MIA phenotypes. At the gene level, SLC25A11 was under-expressed in the cingulate cortex of SSD patients compared to controls [58] and over-expressed in the hippocampus of rats modeling major depressive disorder (MDD) behaviors [59]. The expression of genes in the SLC25 family in the brain was associated with chronic social defeat stress in mice and potentially related to neurological and psychiatric disorders [60].

Ubiquitin carboxyl-terminal hydrolase 30 (USP30, Figure 1) and *n*-ethylmaleimide-sensitive factor (NSF) cofactor p47 (NSFL1C, Figure 1), two genes associated with neurological signal processing, presented major over- and under-expression of alternative isoforms between MIA and control nursed females. The alternative splicing pattern of both genes, including the most under- and over-expressed isoforms in MIA pigs for USP30 (14.7% and 10.2%, respectively) and NSFL1C (11.6% and 2.1%, respectively), are depicted in Figure 1. These profiles could correspond with the role of NSFL1C in the formation of dendritic spines [61] and inhibition of synapse degeneration [62]. Furthermore, the abundance of the NSFL1C protein was lower in the brain of a mouse model of anxiety relative to controls [63]. The impact of MIA on USP30 could be through the disruption of mitophagy and processing of damaged mitochondria [64] because mitochondrial deficits can disrupt neurological function [65].

SH3 and multiple ankyrin repeat domains 1 (SHANK1, Figure 1) and multiple EGF-like domains 8 (MEGF8, Figure 1) presented significant differential splicing between MIA and control weaned females (Table 1, Figure 1). The under-expression of a SHANK1 isoform (5.5%) in MIA relative to control weaned females is aligned with a SHANK1 knockout mouse line that serves as a model of ASD [66]. In addition, SHANK1 was under-expressed in the cerebral cortex of MIA offspring from LPS-challenged rats that

presented neuroinflammation and cortical synaptic deficit [67]. SHANK1 mRNA is expressed predominately in the cerebral cortex, hippocampus, and amygdala and an isoform survey included SHANK1B (lacking the C-terminal SAM domain), SHANK1C (lacking the N-terminal ankyrin repeat domain), and SHANK1D (lacking the ankyrin repeat domain, and SH3 or SAM domains) [68]. The most extreme MEGF8 isoform was under-expressed (8.7%) in MIA relative to control weaned females, and this finding could be correlated with reports of gene variants associated with SSD [69].

The over-expression of a ribosomal protein L28 (RPL28) isoform in MIA relative to control weaned females (2.5%) is aligned reports of over-expression of RPL28 in the frontal cortex of MIA offspring from Poly(I:C)-challenged mice [70]. Likewise, the pattern of the most under-expressed isoform of ATP synthase subunit D, mitochondrial (ATP5H) in MIA relative to control weaned females (2.9%) is consistent with the under-expression of ATP5H in the anterior cingulate gyrus of ASD patients [71]. Moreover, alternative splicing of ATP5H was reported in the hippocampus of aged mice from a line presenting early-onset impaired visuospatial learning [72].

The pattern of the most over-expressed ATPase phospholipid transporting 11B (ATP11B) isoform in MIA relative to control weaned females (5.4%) is consistent with reports of gene over-expression in the prefrontal cortex of MIA offspring from Poly(I:C)-challenged mice [45]. The less extreme under-expression of an ATP11B isoform in MIA females (3.5%) could be associated with the impairment of hippocampal synaptic plasticity observed in an ATP11B knockout mice [73]. Similarly, the profile of the most under-expressed vaccinia related kinase 3 (VRK3) isoform in MIA relative to control weaned females (2.7%) correlates with typical social interactions and repetitive behaviors observed in VRK3 knockout mice that resemble ASD behaviors [74]. The differential alternative splicing of transmembrane 7 superfamily member 2 (TM7SF2) associated with MIA detected in weaned females could be correlated with the differential expression of this gene in SSD-specific neurons [75]. The differential alternative splicing detected in TRNA-YW synthesizing protein 3 homolog (TYW3) and in potassium channel tetramerization domain containing 2 (KCTD2) could be linked to the association between the former gene and susceptibility to ALS and [76] and the alternative splicing of the latter gene uncovered in a mouse line that models ALS [77].

4.2. Differential Alternative Splicing Associated with Maternal Immune Association in Males

Several genes that presented differential alternative splicing between MIA and control nursed males have been previously associated with MIA-associated disorders (Table 2, Figure 2). The under-expression of an isoform in septin-7 (SEPT7, Figure 2) (31.5%) is aligned with reports of gene under-expression in the prefrontal cortex of SSD patients compared to controls [78]. The differential alternative splicing of zinc finger protein 672 (ZNF672, Figure 2) between MIA and control nursed males could be related to reports that this gene contributes to the progression of SSD [79] and that this gene is over-expressed in the blood of SSD patients compared to controls [80].

The detection of differential alternative splicing in the gene potassium voltage-gated channel subfamily A member 6 (KCNA6) among MIA relative to control nursed males (Figure 2) could be correlated with reports that polymorphisms in this gene are associated with SSD [81]. Expression of KCNA6 is developmentally regulated and is correlated with lower neuronal excitability [82].

The differential alternative splicing in myelin transcription factor 1 like (MYT1L) is in agreement with a reported association of this gene with ASD [83], SSD [84], and MDD [85]. The most extreme over-expressed MYT1L isoform was two-fold higher than the most extreme under-expressed isoform, and this pattern correlates with the over-expression of MYT1L in the hippocampus of MIA offspring from influenza-challenged mice [44]. The differential alternative splicing of vasculin (GPBP1) between MIA and control males could refer to the over-expression of this gene in the forebrain of a rat model for depression and mood disorders [86].

The identification of differentially abundant isoforms that map to the genomic region where genes zinc finger protein 74 (ZNF74) and integral membrane protein DGCR2/IDD (DGCR2) are co-located could be related to reports of the association between copy number variation in both genes and higher vulnerability to SSD and ASD [87]. Moreover, polymorphisms in ZNF74 and DGCR2 may contribute to variations in the age-of-onset [88] and overall risk of developing SSD [89,90].

The most extreme over- and under-expressed isoforms from 2',3'-cyclic nucleotide 3' phosphodiesterase (CNP) between MIA and control nursed pigs had similar levels of differential splicing. The opposite isoform profiles reflect the range of CNP findings, including the over-expression of CNP in the hippocampus of MIA offspring from Poly(I:C)-challenged rhesus macaques [47], and the under-expression of CNP in the prefrontal cortex of MIA offspring from Poly(I:C)-challenged mice [45]. Moreover, CNP was under-expressed in the white matter of MIA male mice exposed to inflammatory LPS challenge during development, in the amygdala of patients with major depressive disorder (MDD), and mice exposed to chronic physical and psychological stress [4,91,92].

Consistent with the differential alternative splicing of glial fibrillary acidic protein (GFAP) detected in this study, bias in the expression of GFAP transcripts was reported in a mouse model of ASD [93]. The over-expression of the most extreme GFAP isoform in MIA relative to control nursed males was two-fold higher than that of the isoform with the opposite pattern. This relative pattern agrees with reports that a shorter GFAP isoform was three-fold over-expressed in the cortex of PTEN-knockout mice that present ASD-like behavior compared to controls [93]. In addition, GFAP was over-expressed in the frontal cortex [16] and hippocampus [94] of MIA offspring from LPS-challenged rats and the hippocampus of MIA offspring of mice exposed to the pro-inflammatory cytokine interleukin-6 (IL-6) during gestation [95]. The abundance of the GFAP protein product was higher in the amygdala of MIA offspring from LPS-challenged mice than controls [26].

The differential alternative splicing of the gene neurofilament medium polypeptide (NEFM) is characterized by an isoform under-expressed (9.7%) in MIA relative to control weaned males (Figure 2). This finding is aligned with reports of lower NEFM protein abundance in the prefrontal cortex of MIA offspring from Poly(I:C)-challenged mice [96]. Furthermore, NEFM was under-expressed in the adrenal cortex of 8-week-old female pigs inoculated with LPS and was implicated in AD development [97]. The differential splicing of the neuropeptide precursor corticotropin releasing hormone receptor 1 (CRHR1) detected in MIA weaned pigs (p -value < 0.001) agrees with the differential expression of these gene among male offspring of mice administered Poly(I:C) during gestation [98].

The differential splicing and over-expression of an ADP-ribosylation factor-like protein 4D (ARL4D) isoform (Figure 2) in MIA relative to control weaned males (27.9%) is aligned with the over-expression of ARL4D in the cerebral cortex GABAergic neurons of mice heterozygous for GAD67-GFP knock-in line that presents ADHD and ASD-like behaviors [99]. Likewise, the differential alternative splicing detected in neurocan (NCAN) could be connected with mutations in this gene associated with SSD and bipolar disorder [100]. NCAN variants were associated with limbic gray matter deficits and major depression [101], and a knockout mouse line presented deficits in synaptic plasticity in the hippocampus [102].

The characterization of the alternative splicing of heterogeneous nuclear ribonucleoprotein A2/B1 (HNRNPA2B1) includes subtypes B1 (including all exons), A2 (excluding exon 2), B1b (excluding exon 9), and A2b (excluding exons 2 and 9) [103]. The differential alternative splicing of HNRNPA2B1 detected between MIA and control weaned males could be correlated with reports of associations between mutations and differential expression of this gene and neurodegenerative diseases [103]. Likewise, mutations in TCF25 were associated with ASD, and the reported role of this gene in synaptic function and brain development may align with the differential alternative splicing between MIA and control males [104]. The differential alternative splicing between MIA and control males uncovered for clusterin (CLU) may be related to reports that genetic variants in clusterin (CLU)

were associated with AD development, and alternative transcription start sites have been identified as the driving mechanism for the multiple roles of the resulting transcripts [105].

The pre-mRNA process that regulates the usage of the two alternative 3' exons of CDC42 has been associated with neurogenesis [104] and may be linked to the differential alternative splicing between MIA and control weaned males in males the present study. CDC42 participates in the transportation of GABAergic receptors towards anxiolytic synapses [106] and disruptions in the CDC42 pathway have been noted in the prefrontal cortex of SSD patients [107].

4.3. Functional Analysis of Alternatively Spliced Genes Associated with Maternal Immune Activation

The investigation of pathways encompassing differentially spliced genes between MIA and control pigs yielded insights into the processes potentially affected exposure to inflammatory signals during gestation. The pathway non-alcoholic fatty liver disease (NAFLD; ssc04932; Table 4) was enriched among genes impacted by MIA in nursed females. The detection of the NAFLD pathway is related to the reported association of this pathway with cognitive impairment [108], possibly accelerated brain aging [109], and AD development as indicated by proteomic profiling of mice hippocampi [110].

The Fc gamma R-mediated phagocytosis pathway (ssc04666) was also enriched among genes differentially spliced between MIA and control nursed females. This pathway was enriched among differentially expressed genes in the brains of mice injected with LPS [111] and in patients with AD relative to controls [112]. The enrichment of the endocytosis pathway (ssc04144) in both sexes may be connected to the role of endosomes in neuronal signal transduction, development, dendritic arborization, and axon growth, and guidance [113].

The pathways cGMP-PKG signaling (ssc04022), dopaminergic synapse (ssc04728), amphetamine addiction (ssc05031), ribosome (ssc03010), and calcium signaling (ssc04020, Table 4) encompassed multiple genes presenting differential alternative splicing between MIA and control males. Increased cGMP levels increased synaptic plasticity and attenuated the behavioral deficits observed in offspring mice exposed to Poly(I:C)-elicited MIA [114]. Additionally, increased phosphorylation of PKG targets has been observed in the anterior cingulate cortex of SSD patients compared to controls [115], and PKG may play a role in ASD [116]. The dopaminergic synapse pathway was enriched among genes differentially expressed between rats exposed to LPS-induced MIA and controls [117]. Likewise, changes in the dopaminergic system have been noted in rats exposed to Poly(I:C)-elicited MIA, including a reduction in spontaneous firing of dopaminergic neurons in the ventral tegmental area and an increase in the levels of extracellular dopamine in the nucleus accumbens [118]. The enrichment of the amphetamine addiction pathway is related to the dopamine synapse pathway, as amphetamine is a dopamine agonist that increases extracellular dopamine levels [119]. The enrichment of the amphetamine pathway agrees with evidence of altered amphetamine response in rats exposed to LPS-induced MIA compared to controls [117].

The enrichment of calcium signaling pathway among genes that were alternatively spliced between MIA and control males is supported by evidence that this pathway is dysregulated in individuals with ASD [120]. Moreover, disruption of calcium-ion homeostasis was reported in the neocortex of ASD individuals relative to controls [121]. The detection of differential splicing between MIA and control males annotated to the ribosome pathway could be related to decreased expression of ribosomal genes essential to protein synthesis in the offspring of Poly(I:C)-challenged mice compared to controls [21].

The enrichment of metabolic pathways among genes differentially spliced between MIA and control weaned males is supported by genes including POLR3GL, POLR2E, PRIM1, and AK2. The metabolic pathway includes genes that participate in purine metabolism, amino acids metabolism, and oxidative phosphorylation and this result may indicate a metabolic shift in the pigs exposed to MIA. Previously we reported changes in hepatic metabolites annotated to amino acid metabolic pathways [8], and changes in blood chemical profiles [9] associated with MIA that are aligned with the present alternative splicing results in the amygdala. The over-representation of purine metabolism (e.g.,

POLR3GL, POLR2E, PRIM1, AK2) could be associated with reports that abnormalities in the purine metabolism are common in ASD and that purinergic treatments can alleviate symptoms [122,123]. The over-representation of amino acid metabolism (e.g., HIBCH, AMDHD1, ASL, GATM, SAT1) supports reports that genes in this pathway were disrupted in the offspring of rats challenged with Poly(I:C) during gestation [124]. Likewise, the over-representation of genes annotated to oxidative phosphorylation (e.g., ATP5H, COX6C, NDUFS8) is consistent with the differential expression of genes in the prefrontal cortex of offspring from mice challenged with Poly(I:C) during gestation [125].

5. Conclusions

The present investigation of the effects of MIA on alternative splicing in the amygdala identified significant changes in the relative abundance of transcript isoforms in multiple genes and pathways. The detection of genes encompassing substantially over- and under-expressed isoforms in MIA relative to controls such as MAG, CNP, GFAP, and RPL28 offered insights into some contradictory results from the study of overall gene expression patterns. Our results demonstrate the benefits of studying the impact of MIA on the relative expression profile of isoforms because the characterization of MIA based on overall gene expression patterns may prevent the uncovering of opposite isoform patterns or changes in relative isoform abundance elicited in the amygdala by inflammatory signals during gestation.

The detection of MIA effects on differential splicing that are sex- and weaning stress-dependent highlights the importance of studying the effects of the first challenge resulting in MIA across sexes and in the context of a second challenge. A similar number of genes (approximately 420 genes) presented differential alternative splicing associated with MIA in females and males, and the majority of the differential splicing was detected under weaning stress, relative to nursed conditions. Of these, 30 genes presented MIA-associated differential splicing in two sex or stress groups and two genes (SLC2A11 and MAG) presented differential alternative splicing in three out of four sex-stress groups. The sex- and stress-dependent nature of the differential splicing patterns detected could assist in understanding and developing more individualized effects of MIA on molecular pathways, underlying related physiology, and behavior disorders.

Among the genes presenting differential alternative splicing between MIA and control pigs, several (e.g., PDK2, PRKAR1B, NPTXR, SHANK1, ZNF672, MYT1L, NEFM, and ARL4D) have been previously associated with ASD, SSD, and other behavioral disorders. Likewise, pathways have been previously related with MIA-associated neurodevelopmental and neurodegenerative disorders, including Fc gamma R-mediated phagocytosis, endocytosis, cGMP-PKG signaling pathway, and dopaminergic synapse. The results from this study advance the understanding of the effect of MIA on alternative splicing, including within-gene isoforms presenting opposite association and changes in relative isoform abundance and the characterization of sex- and second stress-dependent MIA effects.

Author Contributions: Conceptualization, R.W.J. and S.L.R.-Z.; Data curation, B.R.S.; Formal analysis, B.R.S.; Funding acquisition, R.W.J. and S.L.R.-Z.; Investigation, M.R.K.-K., H.E.R. and L.A.R.; Project administration, S.L.R.-Z.; Resources, H.E.R., L.A.R., R.W.J. and S.L.R.-Z.; Software, B.R.S.; Supervision, R.W.J. and S.L.R.-Z.; Visualization, B.R.S.; Writing—original draft, B.R.S., M.R.K.-K. and S.L.R.-Z.; Writing—review & editing, B.R.S., M.R.K.-K., H.E.R., L.A.R., R.W.J. and S.L.R.-Z. All authors have read and agreed to the published version of the manuscript.

Funding: This study is supported by USDA NIFA AFRI (grant number 2018-67015-27413) and NIH (grant number P30 DA018310).

Institutional Review Board Statement: The study was conducted according to the guidelines of the Declaration of Helsinki, and approved by the Institutional Review Board and Institutional Animal Care and Use Committee of the University of Illinois (protocol code 20026 approved on March 2018).

Informed Consent Statement: Not applicable.

Data Availability Statement: Data are available from the Gene Expression Omnibus (GEO) database (experiment identifier GSE165059).

Conflicts of Interest: The authors declare no conflict of interest.

References

- Lombardo, M.V.; Moon, H.M.; Su, J.; Palmer, T.D.; Courchesne, E.; Pramparo, T. Maternal immune activation dysregulation of the fetal brain transcriptome and relevance to the pathophysiology of autism spectrum disorder. *Mol. Psychiatry* **2018**, *23*, 1001–1013. [[CrossRef](#)]
- Antonson, A.M.; Lawson, M.A.; Caputo, M.P.; Matt, S.; Leyshon, B.J.; Johnson, R.W. Maternal viral infection causes global alterations in porcine fetal microglia. *Proc. Natl. Acad. Sci. USA* **2019**, *116*, 20190–20200. [[CrossRef](#)] [[PubMed](#)]
- Keever-Keigher, M.R.; Zhang, P.; Bolt, C.R.; Rymut, H.E.; Antonson, A.M.; Corbett, M.P.; Houser, A.K.; Hernandez, A.G.; Southey, B.R.; Rund, L.A.; et al. Interacting impact of maternal inflammatory response and stress on the amygdala transcriptome of pigs. *G3 Genes | Genomes | Genetics* **2021**, *11*, jkab113. [[CrossRef](#)]
- Makinson, R.; Lloyd, K.; Rayasam, A.; McKee, S.; Brown, A.; Barila, G.; Grissom, N.; George, R.; Marini, M.; Fabry, Z.; et al. Intrauterine inflammation induces sex-specific effects on neuroinflammation, white matter, and behavior. *Brain Behav. Immun.* **2017**, *66*, 277–288. [[CrossRef](#)] [[PubMed](#)]
- Rymut, H.E.; Bolt, C.R.; Caputo, M.P.; Houser, A.K.; Antonson, A.M.; Zimmerman, J.D.; Villamil, M.B.; Southey, B.R.; Rund, L.A.; Johnson, R.W.; et al. Long-Lasting Impact of Maternal Immune Activation and Interaction with a Second Immune Challenge on Pig Behavior. *Front. Vet. Sci.* **2020**, *7*, 561151. [[CrossRef](#)] [[PubMed](#)]
- Zolkipli-Cunningham, Z.; Naviaux, J.C.; Nakayama, T.; Hirsch, C.M.; Monk, J.M.; Li, K.; Wang, L.; Le, T.P.; Meinardi, S.; Blake, D.R.; et al. Metabolic and behavioral features of acute hyperpurinergia and the maternal immune activation mouse model of autism spectrum disorder. *PLoS ONE* **2021**, *16*, e0248771. [[CrossRef](#)]
- Rymut, H.E.; Rund, L.A.; Bolt, C.R.; Villamil, M.B.; Bender, D.E.; Southey, B.R.; Johnson, R.W.; Rodriguez-Zas, S.L. Biochemistry and Immune Biomarkers Indicate Interacting Effects of Pre- and Postnatal Stressors in Pigs across Sexes. *Animals* **2021**, *11*, 987. [[CrossRef](#)] [[PubMed](#)]
- Southey, B.R.; Bolt, C.R.; Rymut, H.E.; Keever, M.R.; Ulanov, A.V.; Li, Z.; Rund, L.A.; Johnson, R.W.; Rodriguez-Zas, S.L. Impact of Weaning and Maternal Immune Activation on the Metabolism of Pigs. *Front. Mol. Biosci.* **2021**, *8*, 660764. [[CrossRef](#)] [[PubMed](#)]
- Rymut, H.E.; Rund, L.A.; Bolt, C.R.; Villamil, M.B.; Southey, B.R.; Johnson, R.W.; Rodriguez-Zas, S.L. The Combined Effect of Weaning Stress and Immune Activation during Pig Gestation on Serum Cytokine and Analyte Concentrations. *Animals* **2021**, *11*, 2274. [[CrossRef](#)]
- Bayer, T.A.; Falkai, P.; Maier, W. Genetic and non-genetic vulnerability factors in schizophrenia: The basis of the “Two hit hypothesis”. *J. Psychiatr. Res.* **1999**, *33*, 543–548. [[CrossRef](#)]
- Wang, X.; Hagberg, H.; Nie, C.; Zhu, C.; Ikeda, T.; Mallard, C. Dual Role of Intrauterine Immune Challenge on Neonatal and Adult Brain Vulnerability to Hypoxia-Ischemia. *J. Neuropathol. Exp. Neurol.* **2007**, *66*, 552–561. [[CrossRef](#)] [[PubMed](#)]
- Carlezon, W.A.; Kim, W.; Missig, G.; Finger, B.C.; Landino, S.M.; Alexander, A.J.; Mokler, E.L.; Robbins, J.O.; Li, Y.; Bolshakov, V.Y.; et al. Maternal and early postnatal immune activation produce sex-specific effects on autism-like behaviors and neuroimmune function in mice. *Sci. Rep.* **2019**, *9*, 16928. [[CrossRef](#)] [[PubMed](#)]
- Haida, O.; Al Sagheer, T.; Balbous, A.; Francheteau, M.; Matas, E.; Soria, F.N.; Fernagut, P.O.; Jaber, M. Sex-dependent behavioral deficits and neuropathology in a maternal immune activation model of autism. *Transl. Psychiatry* **2019**, *9*, 124. [[CrossRef](#)] [[PubMed](#)]
- Brown, A.S.; Patterson, P.H. Maternal Infection and Schizophrenia: Implications for Prevention. *Schizophr. Bull.* **2011**, *37*, 284–290. [[CrossRef](#)]
- Openshaw, R.L.; Kwon, J.; McColl, A.; Penninger, J.M.; Cavanagh, J.; Pratt, J.A.; Morris, B.J. JNK signalling mediates aspects of maternal immune activation: Importance of maternal genotype in relation to schizophrenia risk. *J. Neuroinflammation* **2019**, *16*, 18. [[CrossRef](#)]
- Souza, D.F.; Wartchow, K.M.; Lunardi, P.S.; Brolese, G.; Tortorelli, L.S.; Batassini, C.; Biasibetti, R.; Gonçalves, C.-A. Changes in Astroglial Markers in a Maternal Immune Activation Model of Schizophrenia in Wistar Rats are Dependent on Sex. *Front. Cell. Neurosci.* **2015**, *9*, 489. [[CrossRef](#)]
- Xia, Y.; Zhang, Z.; Lin, W.; Yan, J.; Zhu, C.; Yin, D.; He, S.; Su, Y.; Xu, N.; Caldwell, R.W.; et al. Modulating microglia activation prevents maternal immune activation induced schizophrenia-relevant behavior phenotypes via arginase 1 in the dentate gyrus. *Neuropsychopharmacology* **2020**, *45*, 1896–1908. [[CrossRef](#)]
- Knuesel, I.; Chicha, L.; Britschgi, M.; Schobel, S.A.; Bodmer, M.; Hellings, J.A.; Toovey, S.; Prinssen, E.P. Maternal immune activation and abnormal brain development across CNS disorders. *Nat. Rev. Neurol.* **2014**, *10*, 643–660. [[CrossRef](#)] [[PubMed](#)]
- Garbett, K.A.; Hsiao, E.Y.; Kálmán, S.; Patterson, P.H.; Mirnics, K. Effects of maternal immune activation on gene expression patterns in the fetal brain. *Transl. Psychiatry* **2012**, *2*, e98. [[CrossRef](#)]
- Hui, C.W.; Vecchiarelli, H.A.; Gervais, É.; Luo, X.; Michaud, F.; Scheefhals, L.; Bisht, K.; Sharma, K.; Topolnik, L.; Tremblay, M.É. Sex Differences of Microglia and Synapses in the Hippocampal Dentate Gyrus of Adult Mouse Offspring Exposed to Maternal Immune Activation. *Front. Cell. Neurosci.* **2020**, *14*, 331. [[CrossRef](#)] [[PubMed](#)]

21. Kalish, B.T.; Kim, E.; Finander, B.; Duffy, E.E.; Kim, H.; Gilman, C.K.; Yim, Y.S.; Tong, L.; Kaufman, R.J.; Griffith, E.C.; et al. Maternal immune activation in mice disrupts proteostasis in the fetal brain. *Nat. Neurosci.* **2021**, *24*, 204–213. [[CrossRef](#)]
22. Ressler, K.J. Amygdala Activity, Fear, and Anxiety: Modulation by Stress. *Biol. Psychiatry* **2010**, *67*, 1117–1119. [[CrossRef](#)] [[PubMed](#)]
23. Schumann, C.M.; Bauman, M.D.; Amaral, D.G. Abnormal structure or function of the amygdala is a common component of neurodevelopmental disorders. *Neuropsychologia* **2011**, *49*, 745–759. [[CrossRef](#)]
24. Keever, M.R.; Zhang, P.; Bolt, C.R.; Antonson, A.M.; Rymut, H.E.; Caputo, M.P.; Houser, A.K.; Hernandez, A.G.; Southey, B.R.; Rund, L.A.; et al. Lasting and Sex-Dependent Impact of Maternal Immune Activation on Molecular Pathways of the Amygdala. *Front. Neurosci.* **2020**, *14*, 774. [[CrossRef](#)] [[PubMed](#)]
25. Southey, B.R.; Zhang, P.; Keever, M.R.; Rymut, H.E.; Johnson, R.W.; Sweedler, J.V.; Rodriguez-Zas, S.L. Effects of maternal immune activation in porcine transcript isoforms of neuropeptide and receptor genes. *J. Integr. Neurosci.* **2021**, *20*, 21–31. [[CrossRef](#)]
26. O’Loughlin, E.; Pakan, J.M.P.; Yilmazer-Hanke, D.; McDermott, K.W. Acute in utero exposure to lipopolysaccharide induces inflammation in the pre- and postnatal brain and alters the glial cytoarchitecture in the developing amygdala. *J. Neuroinflammation* **2017**, *14*, 212. [[CrossRef](#)] [[PubMed](#)]
27. Li, Y.; Missig, G.; Finger, B.C.; Landino, S.M.; Alexander, A.J.; Mokler, E.L.; Robbins, J.O.; Manasian, Y.; Kim, W.; Kim, K.-S.; et al. Maternal and Early Postnatal Immune Activation Produce Dissociable Effects on Neurotransmission in mPFC–Amygdala Circuits. *J. Neurosci.* **2018**, *38*, 3358–3372. [[CrossRef](#)] [[PubMed](#)]
28. Li, Q.; Lee, J.-A.; Black, D.L. Neuronal regulation of alternative pre-mRNA splicing. *Nat. Rev. Neurosci.* **2007**, *8*, 819–831. [[CrossRef](#)]
29. Zheng, S.; Black, D.L. Alternative pre-mRNA splicing in neurons: Growing up and extending its reach. *Trends Genet.* **2013**, *29*, 442–448. [[CrossRef](#)]
30. Zhang, P.; Southey, B.R.; Rodriguez-Zas, S.L. Co-expression networks uncover regulation of splicing and transcription markers of disease. *EPiC Ser. Comput.* **2020**, *70*, 119–128.
31. Zhang, P.; Southey, B.R.; Sweedler, J.V.; Pradhan, A.; Rodriguez-Zas, S.L. Enhanced Understanding of Molecular Interactions and Function Underlying Pain Processes through Networks of Transcript Isoforms, Genes, and Gene Families. *Adv. Appl. Bioinform. Chem.* **2021**, *14*, 49–69. [[CrossRef](#)] [[PubMed](#)]
32. Voineagu, I.; Wang, X.C.; Johnston, P.; Lowe, J.K.; Tian, Y.; Horvath, S.; Mill, J.; Cantor, R.M.; Blencowe, B.J.; Geschwind, D.H. Transcriptomic analysis of autistic brain reveals convergent molecular pathology. *Nature* **2011**, *474*, 380–384. [[CrossRef](#)] [[PubMed](#)]
33. Morikawa, T.; Manabe, T. Aberrant regulation of alternative pre-mRNA splicing in schizophrenia. *Neurochem. Int.* **2010**, *57*, 691–704. [[CrossRef](#)] [[PubMed](#)]
34. Barry, G.; Briggs, J.A.; Vanichkina, D.P.; Poth, E.M.; Beveridge, N.J.; Ratnu, V.S.; Nayler, S.P.; Nones, K.; Hu, J.; Bredy, T.W.; et al. The long non-coding RNA Gomafu is acutely regulated in response to neuronal activation and involved in schizophrenia-associated alternative splicing. *Mol. Psychiatry* **2014**, *19*, 486–494. [[CrossRef](#)]
35. Dobin, A.; Davis, C.A.; Schlesinger, F.; Drenkow, J.; Zaleski, C.; Jha, S.; Batut, P.; Chaisson, M.; Gingeras, T.R. STAR: Ultrafast universal RNA-seq aligner. *Bioinformatics* **2013**, *29*, 15–21. [[CrossRef](#)]
36. Feng, Y.-Y.; Ramu, A.; Skidmore, Z.L.; Kunisaki, J.; Cotto, K.C.; Griffith, O.L.; Griffith, M. Regtools: Integrated analysis of genomic and transcriptomic data for discovery of mutations associated with aberrant splicing in cancer. *Cancer Res.* **2018**, *78*, 2285. [[CrossRef](#)]
37. Li, Y.I.; Knowles, D.A.; Humphrey, J.; Barbeira, A.N.; Dickinson, S.P.; Im, H.K.; Pritchard, J.K. Annotation-free quantification of RNA splicing using LeafCutter. *Nat. Genet.* **2018**, *50*, 151–158. [[CrossRef](#)]
38. Benjamini, Y.; Hochberg, Y. Controlling the False Discovery Rate: A Practical and Powerful Approach to Multiple Testing. *J. R. Stat. Soc. Ser. B Methodol.* **1995**, *57*, 289–300. [[CrossRef](#)]
39. Huang, D.W.; Sherman, B.T.; Lempicki, R.A. Systematic and integrative analysis of large gene lists using DAVID bioinformatics resources. *Nat. Protoc.* **2009**, *4*, 44. [[CrossRef](#)]
40. Martin, J.; Cooper, M.; Hamshere, M.L.; Pocklington, A.; Scherer, S.W.; Kent, L.; Gill, M.; Owen, M.J.; Williams, N.; O’Donovan, M.C.; et al. Biological Overlap of Attention-Deficit/Hyperactivity Disorder and Autism Spectrum Disorder: Evidence from Copy Number Variants. *J. Am. Acad. Child Adolesc. Psychiatry* **2014**, *53*, 761–770. [[CrossRef](#)]
41. Bassett, A.S.; Lowther, C.; Merico, D.; Costain, G.; Chow, E.W.C.; van Amelsvoort, T.; McDonald-McGinn, D.; Gur, R.E.; Swillen, A.; Bree, M.V.D.; et al. Rare Genome-Wide Copy Number Variation and Expression of Schizophrenia in 22q11.2 Deletion Syndrome. *Am. J. Psychiatry* **2017**, *174*, 1054–1063. [[CrossRef](#)] [[PubMed](#)]
42. Aberg, K.; Saetre, P.; Jareborg, N.; Jazin, E. Human QKI, a potential regulator of mRNA expression of human oligodendrocyte-related genes involved in schizophrenia. *Proc. Natl. Acad. Sci. USA* **2006**, *103*, 7482–7487. [[CrossRef](#)]
43. Zhang, X.-F.; Chen, T.; Yan, A.F.; Xiao, J.; Xie, Y.-L.; Yuan, J.; Chen, P.; Wong, A.O.-L.; Zhang, Y.; Wong, N.-K. Poly(I:C) Challenge Alters Brain Expression of Oligodendroglia-Related Genes of Adult Progeny in a Mouse Model of Maternal Immune Activation. *Front. Mol. Neurosci.* **2020**, *13*, 115. [[CrossRef](#)]
44. Farrelly, L.; Foeking, M.; Piontkewitz, Y.; Dicker, P.; English, J.; Wynne, K.; Cannon, M.; Cagney, G.; Cotter, D.R. Maternal Immune Activation Induces Changes in Myelin and Metabolic Proteins, Some of Which Can Be Prevented with Risperidone in Adolescence. *Dev. Neurosci.* **2015**, *37*, 43–55. [[CrossRef](#)] [[PubMed](#)]

45. Richetto, J.; Chesters, R.; Cattaneo, A.; Labouesse, M.A.; Gutierrez, A.M.C.; Wood, T.C.; Luoni, A.; Meyer, U.; Vernon, A.; Riva, M.A. Genome-Wide Transcriptional Profiling and Structural Magnetic Resonance Imaging in the Maternal Immune Activation Model of Neurodevelopmental Disorders. *Cereb. Cortex* **2016**, *27*, 3397–3413. [[CrossRef](#)]
46. Fatemi, S.H.; Folsom, T.D.; Reutiman, T.J.; Abu-Odeh, D.; Mori, S.; Huang, H.; Oishi, K. Abnormal expression of myelination genes and alterations in white matter fractional anisotropy following prenatal viral influenza infection at E16 in mice. *Schizophr. Res.* **2009**, *112*, 46–53. [[CrossRef](#)] [[PubMed](#)]
47. Page, N.F.; Gandal, M.; Estes, M.; Cameron, S.; Buth, J.; Parhami, S.; Ramaswami, G.; Murray, K.; Amaral, D.G.; van de Water, J.A.; et al. Alterations in retrotransposition, synaptic connectivity, and myelination implicated by transcriptomic changes following maternal immune activation in non-human primates. *Biol. Psychiatry* **2020**, *89*, 896–910. [[CrossRef](#)]
48. Strutz-Seebohm, N.; Seebohm, G.; Mack, A.F.; Wagner, H.-J.; Just, L.; Skutella, T.; Lang, U.E.; Henke, G.; Striegel, M.; Hollmann, M.; et al. Regulation of GluR1 abundance in murine hippocampal neurones by serum-and glucocorticoid-inducible kinase 3. *J. Physiol.* **2005**, *565*, 381–390. [[CrossRef](#)] [[PubMed](#)]
49. Hoeffer, C.A.; Klann, E. mTOR signaling: At the crossroads of plasticity, memory and disease. *Trends Neurosci.* **2010**, *33*, 67–75. [[CrossRef](#)]
50. Gipson, T.T.; Johnston, M.V. Plasticity and mTOR: Towards Restoration of Impaired Synaptic Plasticity in mTOR-Related Neurogenetic Disorders. *Neural Plast.* **2012**. [[CrossRef](#)]
51. Nardone, S.; Sams, D.S.; Zito, A.; Reuveni, E.; Elliott, E. Dysregulation of Cortical Neuron DNA Methylation Profile in Autism Spectrum Disorder. *Cereb. Cortex* **2017**, *27*, 5739–5754. [[CrossRef](#)] [[PubMed](#)]
52. Cohen, O.S.; McCoy, S.Y.; Middleton, F.A.; Bialosuknia, S.; Zhang-James, Y.; Liu, L.; Tsuang, M.T.; Faraone, S.V.; Glatt, S.J. Transcriptomic analysis of postmortem brain identifies dysregulated splicing events in novel candidate genes for schizophrenia. *Schizophr. Res.* **2012**, *142*, 188–199. [[CrossRef](#)] [[PubMed](#)]
53. Pelkey, K.A.; Barksdale, E.; Craig, M.T.; Yuan, X.Q.; Sukumaran, M.; Vargish, G.A.; Mitchell, R.M.; Wyeth, M.S.; Petralia, R.S.; Chittajallu, R.; et al. Pentraxins Coordinate Excitatory Synapse Maturation and Circuit Integration of Parvalbumin Interneurons. *Neuron* **2016**, *90*, 661. [[CrossRef](#)]
54. Ripke, S.; Neale, B.M.; Corvin, A.; Walters, J.T.; Farh, K.H.; Holmans, P.A.; Lee, P.; Bulik-Sullivan, B.; Collier, D.A.; Huang, H.; et al. Biological insights from 108 schizophrenia-associated genetic loci. *Nature* **2014**, *511*, 421. [[CrossRef](#)]
55. Ronemus, M.; Iossifov, I.; Levy, D.; Wigler, M. The role of de novo mutations in the genetics of autism spectrum disorders. *Nat. Rev. Genet.* **2014**, *15*, 133–141. [[CrossRef](#)] [[PubMed](#)]
56. Campbell, M.; Jahanshad, N.; Mufford, M.; Choi, K.W.; Lee, P.; Ramesar, R.; Smoller, J.W.; Thompson, P.; Stein, D.J.; Dalvie, S. Overlap in genetic risk for cross-disorder vulnerability to mental disorders and genetic risk for altered subcortical brain volumes. *J. Affect. Disord.* **2021**, *282*, 740–756. [[CrossRef](#)]
57. Moskal, J.R.; Burgdorf, J.; Kroes, R.A.; Brudzynski, S.M.; Panksepp, J. A novel NMDA receptor glycine-site partial agonist, GLYX-13, has therapeutic potential for the treatment of autism. *Neurosci. Biobehav. Rev.* **2011**, *35*, 1982–1988. [[CrossRef](#)]
58. Föcking, M.; Lopez, L.M.; English, J.A.; Dicker, P.; Wolff, A.; Brindley, E.; Wynne, K.; Cagney, G.; Cotter, D.R. Proteomic and genomic evidence implicates the postsynaptic density in schizophrenia. *Mol. Psychiatry* **2015**, *20*, 424–432. [[CrossRef](#)]
59. Han, X.; Shao, W.; Liu, Z.; Fan, S.-H.; Yu, J.; Chen, J.; Qiao, R.; Zhou, J.; Xie, P. iTRAQ-based quantitative analysis of hippocampal postsynaptic density-associated proteins in a rat chronic mild stress model of depression. *Neuroscience* **2015**, *298*, 220–292. [[CrossRef](#)]
60. Babenko, V.N.; Smagin, D.A.; Galyamina, A.G.; Kovalenko, I.L.; Kudryavtseva, N.N. Altered Slc25 family gene expression as markers of mitochondrial dysfunction in brain regions under experimental mixed anxiety/depression-like disorder. *BMC Neurosci.* **2018**, *19*, 79. [[CrossRef](#)] [[PubMed](#)]
61. Shih, Y.-T.; Hsueh, Y.-P. VCP and ATL1 regulate endoplasmic reticulum and protein synthesis for dendritic spine formation. *Nat. Commun.* **2016**, *7*, 11020. [[CrossRef](#)] [[PubMed](#)]
62. Wang, K.Z.Q.; Steer, E.; Otero, P.A.; Bateman, N.W.; Cheng, M.H.; Scott, A.L.; Wu, C.; Bahar, I.; Shih, Y.-T.; Hsueh, Y.-P.; et al. PINK1 Interacts with VCP/p97 and Activates PKA to Promote NSFL1C/p47 Phosphorylation and Dendritic Arborization in Neurons. *eNeuro* **2018**, *5*, 0466. [[CrossRef](#)] [[PubMed](#)]
63. Szegő, É.M.; Janáky, T.; Szabó, Z.; Csorba, A.; Kompagne, H.; Müller, G.; Lévy, G.; Simor, A.; Juhász, G.; Kékesi, K.A. A mouse model of anxiety molecularly characterized by altered protein networks in the brain proteome. *Eur. Neuropsychopharmacol.* **2010**, *20*, 96–111. [[CrossRef](#)] [[PubMed](#)]
64. Bingol, B.; Tea, J.S.; Phu, L.; Reichelt, M.; Bakalarski, C.E.; Song, Q.H.; Foreman, O.; Kirkpatrick, D.S.; Sheng, M.G. The mitochondrial deubiquitinase USP30 opposes parkin-mediated mitophagy. *Nat. Cell Biol.* **2014**, *510*, 370–375. [[CrossRef](#)] [[PubMed](#)]
65. Abou-Sleiman, P.M.; Muqit, M.K.; Wood, N.W. Expanding insights of mitochondrial dysfunction in Parkinson's disease. *Nat. Rev. Neurosci.* **2006**, *7*, 207–219. [[CrossRef](#)]
66. Malkova, N.V.; Yu, C.Z.; Hsiao, E.Y.; Moore, M.J.; Patterson, P.H. Maternal immune activation yields offspring displaying mouse versions of the three core symptoms of autism. *Brain Behav. Immun.* **2012**, *26*, 607–616. [[CrossRef](#)]
67. Cieślak, M.; Gaśowska-Dobrowolska, M.; Jeśko, H.; Czapski, G.A.; Wilkaniec, A.; Zawadzka, A.; Dominiak, A.; Polowy, R.; Filipkowski, R.K.; Boguszewski, P.M.; et al. Maternal Immune Activation Induces Neuroinflammation and Cortical Synaptic Deficits in the Adolescent Rat Offspring. *Int. J. Mol. Sci.* **2020**, *21*, 4097. [[CrossRef](#)]

68. Wan, L.; Liu, D.; Xiao, W.-B.; Zhang, B.-X.; Yan, X.-X.; Luo, Z.-H.; Xiao, B. Association of SHANK Family with Neuropsychiatric Disorders: An Update on Genetic and Animal Model Discoveries. *Cell. Mol. Neurobiol.* **2021**, 1–21. [\[CrossRef\]](#)
69. Rhoades, R.; Jackson, F.; Teng, S. Discovery of rare variants implicated in schizophrenia using next-generation sequencing. *J. Transl. Genet. Genom.* **2019**, *3*, 1–20. [\[CrossRef\]](#)
70. Amodeo, D.A.; Lai, C.-Y.; Hassan, O.; Mukamel, E.A.; Behrens, M.M.; Powell, S.B. Maternal immune activation impairs cognitive flexibility and alters transcription in frontal cortex. *Neurobiol. Dis.* **2019**, *125*, 211–218. [\[CrossRef\]](#)
71. Legido, A.; Jethva, R.; Goldenthal, M.J. Mitochondrial Dysfunction in Autism. *Semin. Pediatr. Neurol.* **2013**, *20*, 163–175. [\[CrossRef\]](#)
72. Yang, J.; Long, Y.; Xu, D.-M.; Zhu, B.-L.; Deng, X.-J.; Yan, Z.; Sun, F.; Chen, G.-J. Age- and Nicotine-Associated Gene Expression Changes in the Hippocampus of APP/PS1 Mice. *J. Mol. Neurosci.* **2019**, *69*, 608–622. [\[CrossRef\]](#)
73. Wang, J.; Li, W.; Zhou, F.; Feng, R.; Wang, F.; Zhang, S.; Li, J.; Li, Q.; Wang, Y.; Xie, J.; et al. ATP11B deficiency leads to impairment of hippocampal synaptic plasticity. *J. Mol. Cell Biol.* **2019**, *11*, 688–702. [\[CrossRef\]](#)
74. Emili, M.; Guidi, S.; Uguagliati, B.; Giacomini, A.; Bartesaghi, R.; Stagni, F. Treatment with the flavonoid 7,8-Dihydroxyflavone: A promising strategy for a constellation of body and brain disorders. *Crit. Rev. Food Sci. Nutr.* **2020**, *10*, 1–38. [\[CrossRef\]](#) [\[PubMed\]](#)
75. Lin, M.; Zhao, D.; Hrabovsky, A.; Pedrosa, E.; Zheng, D.; Lachman, H.M. Heat Shock Alters the Expression of Schizophrenia and Autism Candidate Genes in an Induced Pluripotent Stem Cell Model of the Human Telencephalon. *PLoS ONE* **2014**, *9*, e94968. [\[CrossRef\]](#) [\[PubMed\]](#)
76. Wei, L.; Tian, Y.; Chen, Y.; Wei, Q.; Chen, F.; Cao, B.; Wu, Y.; Zhao, B.; Chen, X.; Xie, C.; et al. Identification of TYW3/CRYZ and FGD4 as susceptibility genes for amyotrophic lateral sclerosis. *Neurol. Genet.* **2019**, *5*, e375. [\[CrossRef\]](#) [\[PubMed\]](#)
77. Wu, L.-S.; Cheng, W.-C.; Chen, C.-Y.; Wu, M.-C.; Wang, Y.-C.; Tseng, Y.-H.; Chuang, T.-J.; Shen, C.-K.J. Transcriptomopathies of pre- and post-symptomatic frontotemporal dementia-like mice with TDP-43 depletion in forebrain neurons. *Acta Neuropathol. Commun.* **2019**, *7*, 50. [\[CrossRef\]](#)
78. Ide, M.; Lewis, D.A. Altered Cortical CDC42 Signaling Pathways in Schizophrenia: Implications for Dendritic Spine Deficits. *Biol. Psychiatry* **2010**, *68*, 25–32. [\[CrossRef\]](#) [\[PubMed\]](#)
79. Yazdani, A.; Mendez-Giraldez, R.; Yazdani, A.; Kosorok, M.R.; Roussos, P. Differential gene regulatory pattern in the human brain from schizophrenia using transcriptomic-causal network. *BMC Bioinform.* **2020**, *21*, 469. [\[CrossRef\]](#)
80. Gardiner, E.J.; Cairns, M.J.; Liu, B.; Beveridge, N.J.; Carr, V.; Kelly, B.; Scott, R.J.; Tooney, P.A.; Bank, A.S.R. Gene expression analysis reveals schizophrenia-associated dysregulation of immune pathways in peripheral blood mononuclear cells. *J. Psychiatr. Res.* **2013**, *47*, 425–437. [\[CrossRef\]](#)
81. Lee, Y.H.; Kim, J.-H.; Song, G.G. Pathway analysis of a genome-wide association study in schizophrenia. *Gene* **2013**, *525*, 107–115. [\[CrossRef\]](#)
82. Okaty, B.W.; Miller, M.N.; Sugino, K.; Hempel, C.M.; Nelson, S.B. Transcriptional and Electrophysiological Maturation of Neocortical Fast-Spiking GABAergic Interneurons. *J. Neurosci.* **2009**, *29*, 7040–7052. [\[CrossRef\]](#)
83. Garbett, K.; Ebert, P.J.; Mitchell, A.; Lintas, C.; Manzi, B.; Mirnics, K.; Persico, A.M. Immune transcriptome alterations in the temporal cortex of subjects with autism. *Neurobiol. Dis.* **2008**, *30*, 303–311. [\[CrossRef\]](#)
84. Vrijenhoek, T.; Buizer-Voskamp, J.E.; van der Stelt, I.; Strengman, E.; Sabatti, C.; van Kessel, A.G.; Brunner, H.G.; Ophoff, R.A.; Veltman, J.A. Recurrent CNVs Disrupt Three Candidate Genes in Schizophrenia Patients. *Am. J. Hum. Genet.* **2008**, *83*, 504–510. [\[CrossRef\]](#)
85. Wang, T.; Zeng, Z.; Li, T.; Liu, J.; Li, J.; Li, Y.; Zhao, Q.; Wei, Z.; Wang, Y.; Li, B.; et al. Common SNPs in Myelin Transcription Factor 1-Like (MYT1L): Association with Major Depressive Disorder in the Chinese Han Population. *PLoS ONE* **2010**, *5*, e13662. [\[CrossRef\]](#) [\[PubMed\]](#)
86. Lagus, M.; Gass, N.; Saharinen, J.; Saarela, J.; Porkka-Heiskanen, T.; Paunio, T. Gene expression patterns in a rodent model for depression. *Eur. J. Neurosci.* **2010**, *31*, 1465–1473. [\[CrossRef\]](#) [\[PubMed\]](#)
87. Birnbaum, R.; Jaffe, A.E.; Hyde, T.M.; Kleinman, J.E.; Weinberger, D.R. Prenatal Expression Patterns of Genes Associated with Neuropsychiatric Disorders. *Am. J. Psychiatry* **2014**, *171*, 758–767. [\[CrossRef\]](#) [\[PubMed\]](#)
88. Takase, K.; Ohtsuki, T.; Migita, O.; Toru, M.; Inada, T.; Yamakawa-Kobayashi, K.; Arinami, T. Association of ZNF74 gene genotypes with age-at-onset of schizophrenia. *Schizophr. Res.* **2001**, *52*, 161–165. [\[CrossRef\]](#)
89. Shifman, S.; Levit, A.; Chen, M.-L.; Chen, C.-H.; Bronstein, M.; Weizman, A.; Yakir, B.; Navon, R.; Darvasi, A. A complete genetic association scan of the 22q11 deletion region and functional evidence reveal an association between DGCR2 and schizophrenia. *Qual. Life Res.* **2006**, *120*, 160–170. [\[CrossRef\]](#)
90. Horowitz, A.; Shifman, S.; Rivlin, N.; Pisanté, A.; Darvasi, A. A survey of the 22q11 microdeletion in a large cohort of schizophrenia patients. *Schizophr. Res.* **2005**, *73*, 263–267. [\[CrossRef\]](#)
91. Sibille, E.; Wang, Y.J.; Joeyen-Waldorf, J.; Gaiteri, C.; Surget, A.; Oh, S.; Belzung, C.; Tseng, G.C.; Lewis, D.A. A Molecular Signature of Depression in the Amygdala. *Am. J. Psychiatry* **2009**, *166*, 1011–1024. [\[CrossRef\]](#)
92. Sun, Y.; Lu, W.; Du, K.X.; Wang, J.-H. microRNA and mRNA profiles in the amygdala are relevant to fear memory induced by physical or psychological stress. *J. Neurophysiol.* **2019**, *122*, 1002–1022. [\[CrossRef\]](#)
93. Thacker, S.; Sefyi, M.; Eng, C. Alternative splicing landscape of the neural transcriptome in a cytoplasmic-predominant Pten expression murine model of autism-like Behavior. *Transl. Psychiatry* **2020**, *10*, 380. [\[CrossRef\]](#)
94. Hao, L.Y.; Hao, X.Q.; Li, S.H.; Li, X.H. Prenatal exposure to lipopolysaccharide results in cognitive deficits in age-increasing offspring rats. *Neuroscience* **2010**, *166*, 763–770. [\[CrossRef\]](#)

95. Samuelsson, A.-M.; Jennische, E.; Hansson, H.-A.; Holmång, A. Prenatal exposure to interleukin-6 results in inflammatory neurodegeneration in hippocampus with NMDA/GABAA dysregulation and impaired spatial learning. *Am. J. Physiol. Integr. Comp. Physiol.* **2006**, *290*, R1345–R1356. [[CrossRef](#)]
96. Kim, H.-J.; Won, H.; Im, J.; Lee, H.; Park, J.; Lee, S.; Kim, Y.-O.; Kim, H.-K.; Kwon, J.-T. Effects of Panax ginseng C.A. Meyer extract on the offspring of adult mice with maternal immune activation. *Mol. Med. Rep.* **2018**, *18*, 3834–3842. [[CrossRef](#)]
97. Paukszto, L.; Mikolajczyk, A.; Szeszko, K.; Smolinska, N.; Jastrzębski, J.P.; Kaminski, T. Transcription analysis of the response of the porcine adrenal cortex to a single subclinical dose of lipopolysaccharide from Salmonella Enteritidis. *Int. J. Biol. Macromol.* **2019**, *141*, 1228–1245. [[CrossRef](#)]
98. Zhao, X.; Mohammed, R.; Tran, H.; Erickson, M.; Kentner, A.C. Poly (I:C)-induced maternal immune activation modifies ventral hippocampal regulation of stress reactivity: Prevention by environmental enrichment. *Brain Behav. Immun.* **2021**, *95*, 203–215. [[CrossRef](#)]
99. Fukumoto, K.; Tamada, K.; Toya, T.; Nishino, T.; Yanagawa, Y.; Takumi, T. Identification of genes regulating GABAergic interneuron maturation. *Neurosci. Res.* **2018**, *134*, 18–29. [[CrossRef](#)]
100. Jang, D.G.; Sim, H.J.; Song, E.K.; Kwon, T.; Park, T.J. Extracellular matrixes and neuroinflammation. *BMB Rep.* **2020**, *53*, 491–499. [[CrossRef](#)]
101. Dannlowski, U.; Kugel, H.; Grotegerd, D.; Redlich, R.; Suchy, J.; Opel, N.; Suslow, T.; Konrad, C.; Ohrmann, P.; Bauer, J.; et al. NCAN Cross-Disorder Risk Variant Is Associated with Limbic Gray Matter Deficits in Healthy Subjects and Major Depression. *Neuropsychopharmacology* **2015**, *40*, 2510–2516. [[CrossRef](#)] [[PubMed](#)]
102. Zhou, X.-H.; Brakebusch, C.; Matthies, H.; Oohashi, T.; Hirsch, E.; Moser, M.; Krug, M.; Seidenbecher, C.I.; Boeckers, T.M.; Rauch, U.; et al. Neurocan Is Dispensable for Brain Development. *Mol. Cell. Biol.* **2001**, *21*, 4460–4469. [[CrossRef](#)]
103. Liu, Y.; Shi, S.-L. The roles of hnRNP A2 / B1 in RNA biology and disease. *Wiley Interdiscip. Rev. RNA* **2021**, *12*, e1612. [[CrossRef](#)] [[PubMed](#)]
104. Park, D.I. Chapter Three—Genomics, transcriptomics, proteomics and big data analysis in the discovery of new diagnostic markers and targets for therapy development. *Prog. Mol. Bio. Translat. Sci.* **2020**, *173*, 61–90.
105. Szymanski, M.; Wang, R.; Bassett, S.S.; Avramopoulos, D. Alzheimer’s risk variants in the clusterin gene are associated with alternative splicing. *Transl. Psychiatry* **2011**, *1*, e18. [[CrossRef](#)] [[PubMed](#)]
106. Soreq, L.; Guffanti, A.; Salomonis, N.; Simchovitz, A.; Israel, Z.; Bergman, H.; Soreq, H. Long Non-Coding RNA and Alternative Splicing Modulations in Parkinson’s Leukocytes Identified by RNA Sequencing. *PLoS Comput. Biol.* **2014**, *10*, e1003517. [[CrossRef](#)]
107. Volk, D.W. Role of microglia disturbances and immune-related marker abnormalities in cortical circuitry dysfunction in schizophrenia. *Neurobiol. Dis.* **2017**, *99*, 58–65. [[CrossRef](#)]
108. Seo, S.W.; Gottesman, R.F.; Clark, J.M.; Hernaez, R.; Chang, Y.; Kim, C.; Ha, K.H.; Guallar, E.; Lazo, M. Nonalcoholic fatty liver disease is associated with cognitive function in adults. *Neurology* **2016**, *86*, 1136–1142. [[CrossRef](#)] [[PubMed](#)]
109. Weinstein, G.; Zelber-Sagi, S.; Preis, S.R.; Beiser, A.S.; DeCarli, C.; Speliotes, E.K.; Satizabal, C.L.; Vasan, R.S.; Seshadri, S. Association of Nonalcoholic Fatty Liver Disease with Lower Brain Volume in Healthy Middle-aged Adults in the Framingham Study. *JAMA Neurol.* **2018**, *75*, 97–104. [[CrossRef](#)] [[PubMed](#)]
110. He, K.W.; Nie, L.L.; Zhou, Q.; Rahman, S.U.; Liu, J.J.; Yang, X.F.; Li, S.P. Proteomic Profiles of the Early Mitochondrial Changes in APP/PS1 and ApoE4 Transgenic Mice Models of Alzheimer’s Disease. *J. Proteome Res.* **2019**, *18*, 2632–2642. [[CrossRef](#)] [[PubMed](#)]
111. Gao, Y.; Liang, X.; Ren, Z.; Li, Y.; Yang, X. Systematic search for schizophrenia pathways sensitive to perturbation by immune activation. *bioRxiv* **2019**, 730655. [[CrossRef](#)]
112. Kong, W.; Mou, X.; Zhang, N.; Zeng, W.; Li, S.; Yang, Y. The Construction of Common and Specific Significance Subnetworks of Alzheimer’s Disease from Multiple Brain Regions. *BioMed Res. Int.* **2015**, *2015*, 394260. [[CrossRef](#)] [[PubMed](#)]
113. Cosker, K.E.; Segal, R.A. Neuronal Signaling through Endocytosis. *Cold Spring Harb. Perspect. Biol.* **2014**, *6*, a020669. [[CrossRef](#)] [[PubMed](#)]
114. Richetto, J.; Scarborough, J.; Arban, R.; Dorner-Ciossek, C.; Rosenbrock, H.; Meyer, U. F21. The Phosphodiesterase-9 Inhibitor Bi 409306 Attenuates Social Interaction and Dopaminergic Deficits in Adult Offspring of Poly (I:C)-Based Maternal Immune Activation Neurodevelopmental Mouse Model. *Schizophr. Bull.* **2019**, *45*, S262. [[CrossRef](#)]
115. McGuire, J.L.; Hammond, J.H.; Yates, S.D.; Chen, D.Q.; Haroutunian, V.; Meador-Woodruff, J.H.; McCullumsmith, R.E. Altered serine/threonine kinase activity in schizophrenia. *Brain Res.* **2014**, *1568*, 42–54. [[CrossRef](#)] [[PubMed](#)]
116. Blakely, R.D.; DeFelice, L.J.; Galli, A. Biogenic Amine Neurotransmitter Transporters: Just When You Thought You Knew them. *Physiology* **2005**, *20*, 225–231. [[CrossRef](#)]
117. Straley, M.E.; van Oeffelen, W.; Theze, S.; Sullivan, A.; Mahony, S.O.; Cryan, J.F.; O’Keefe, G.W. Distinct alterations in motor & reward seeking behavior are dependent on the gestational age of exposure to LPS-induced maternal immune activation. *Brain Behav. Immun.* **2017**, *63*, 21–34. [[CrossRef](#)]
118. Luchicchi, A.; Lecca, S.; Melis, M.; de Felice, M.; Cadeddu, F.; Frau, R.; Muntoni, A.L.; Fadda, P.; Devoto, P.; Pistis, M. Maternal Immune Activation Disrupts Dopamine System in the Offspring. *Int. J. Neuropsychopharmacol.* **2016**, *19*, pyw007. [[CrossRef](#)] [[PubMed](#)]
119. Fleckenstein, A.E.; Volz, T.J.; Riddle, E.L.; Gibb, J.W.; Hanson, G.R. New Insights into the Mechanism of Action of Amphetamines. *Annu. Rev. Pharmacol. Toxicol.* **2007**, *47*, 681–698. [[CrossRef](#)]

120. Wen, Y.; Alshikho, M.J.; Herbert, M.R. Pathway Network Analyses for Autism Reveal Multisystem Involvement, Major Overlaps with Other Diseases and Convergence upon MAPK and Calcium Signaling. *PLoS ONE* **2016**, *11*, e0153329. [[CrossRef](#)]
121. Palmieri, L.; Papaleo, V.; Porcelli, V.; Scarcia, P.; Gaita, L.; Sacco, R.; Hager, J.; Rousseau, F.; Curatolo, P.; Manzi, B.; et al. Altered calcium homeostasis in autism-spectrum disorders: Evidence from biochemical and genetic studies of the mitochondrial aspartate/glutamate carrier AGC1. *Mol. Psychiatry* **2010**, *15*, 38–52. [[CrossRef](#)]
122. Naviaux, R.K.; Zolkipli, Z.; Wang, L.; Nakayama, T.; Naviaux, J.C.; Le, T.P.; Schuchbauer, M.A.; Rogac, M.; Tang, Q.; Dugan, L.L.; et al. Antipurinergic Therapy Corrects the Autism-Like Features in the Poly(IC) Mouse Model. *PLoS ONE* **2013**, *8*, e57380. [[CrossRef](#)]
123. Naviaux, J.C.; Schuchbauer, M.A.; Li, K.; Wang, L.; Risbrough, V.B.; Powell, S.B.; Naviaux, R.K. Reversal of autism-like behaviors and metabolism in adult mice with single-dose antipurinergic therapy. *Transl. Psychiatry* **2014**, *4*, e400. [[CrossRef](#)] [[PubMed](#)]
124. McColl, E.R.; Piquette-Miller, M. Poly(I:C) alters placental and fetal brain amino acid transport in a rat model of maternal immune activation. *Am. J. Reprod. Immunol.* **2019**, *81*, e13115. [[CrossRef](#)] [[PubMed](#)]
125. Mueller, F.S.; Scarborough, J.; Schalbetter, S.M.; Richetto, J.; Kim, E.; Couch, A.; Yee, Y.; Lerch, J.P.; Vernon, A.C.; Weber-Stadlbauer, U.; et al. Behavioral, neuroanatomical, and molecular correlates of resilience and susceptibility to maternal immune activation. *Mol. Psychiatry* **2021**, *26*, 396–410. [[CrossRef](#)]